WPBB-PR(17) 17871

I Palermo et al.

Divertor options impact on DEMO nuclear performances

Preprint of Paper to be submitted for publication in
Fusion Engineering and Design

This work has been carried out within the framework of the EUROfusion Consortium and has received funding from the Euratom research and training programme 2014-2018 under grant agreement No 633053. The views and opinions expressed herein do not necessarily reflect those of the European Commission.

Divertor options impact on DEMO nuclear performances

Iole Palermo[1], Rosaria Villari[2], Angel Ibarra[1]

[1]CIEMAT, Fusion Technology Division, Avda. Complutense 40, 28040-Madrid, SPAIN, *iole.palermo@ciemat.es

[2] ENEA, Fusion and Technology for Nuclear Safety and Security Department, ENEA C. R. Frascati, via E. Fermi 45, 00044 Frascati (Roma), Italy

The present paper addresses the impact of the divertor option on the nuclear performances of the Demonstration fusion reactor (DEMO). As the effect of the number and size of the divertor has been already evaluated, in this work the focus has been posed on the composition in terms of amount of cooling inside the divertor cassette. Transport responses, as the Tritium breeding ratio (TBR), neutron and gamma fluxes and spectra inside the plasma chamber, as well as activation responses such as shutdown dose rate, decay gamma fluxes and heating have been evaluated for two different blanket concepts of the future European DEMO reactor: DCLL and WCLL. Three different divertor compositions have been tested demonstrating the importance of this component not only locally but in the global radiation field. The transport analysis has been performed with the Monte Carlo code MCNP5 and the JEFF3.1.1 and JEFF3.2 data libraries. The activation responses calculated using Advanced D1S method have been recently assessed and summarized in the present paper.

1. Introduction

Tritium self-sufficiency is a prior requirement in a fusion demonstrative (DEMO) power plant.

Many efforts have been done in the past years [1][2][3] for the improvement in the prediction of the Tritium Breeding Ratio (TBR), which is the measure for the self-sufficiency.

With the course of time, the more sophisticated analyses, tools and data libraries have allowed to consider less margin of uncertainties in the TBR target value. Currently, for the fusion power demonstration reactor DEMO developed in the framework of the EU fusion roadmap "Horizon 2020", the requirement for the overall TBR is 1.1 [4] that is the target to be achieved for the sustainability and reliability of the plant. Indeed, due to the various uncertainties and plant-internal losses occurring during DEMO operation, a margin of 10% (for a final net TBR $\geq$ 1.0) is required.

All the margins of uncertainties that could occurs have been exhaustively characterized but the uncertainties due to specific engineering design assumptions are extremely difficult to quantify and predict since they usually change with the design progress. Generally, the TBR performance degrades as the design becomes more detailed. To account for this, it would be safe to include an uncertainty margin of 2–3% [3]. This is, however, not mandatory and might be neglected if one can be sure the design is technically mature.

In the prediction of the TBR some aspects of the design have not been sufficiently considered so far, as the case of the influence of the divertor as addressed in the present paper. The impact on the TBR due to the loss of blanket coverage related to the space occupied by the divertor have been recently published [5][6]. Three options: no divertor, 1 divertor (Single Null) and 2 divertors (Double Null) have been considered in these studies, evidencing a strong relation among the loss of blanket coverage area with the loss of TBR.

However, the impact on TBR and relevant nuclear responses is not only due to the geometrical loss of blanket materials but, considering the same dimensions, the divertor compositions could impact the radiation field inside the plasma chambers. The present paper deals with such problem and it is focused on the relevance of the material composition of the Divertor cassette on TBR performances and on the radiation environment. The divertor composition impacts also on activation of in-vessel components and this effect, recently introduced in [7], is detailed in this paper.

The methodology (DEMO designs, divertor designs, codes, libraries, irradiation scenario, etc.) applied for the execution of the activity is described in Section 2. The results of the impact of divertor composition on transport and activation responses are analyzed in Section 3.

2. Methodology, assumptions and input data

2.1 The DEMO design

A lot of efforts have been done in the recent years for the development of a DEMO conceptual design with special attention: 1) to the Tritium Breeding Ratio target fulfilment for a sustainable operation of the plant and 2) to the use of low activation materials to demonstrate that the tangible part of this energy source, as are the materials of a fusion reactor, is really committed to the environment.

2.1.1 DCLL and WCLL BB designs

As part of the first objective a special R&D Work Package in the framework of the EUROfusion

author's email: iole.palermo@ciemat.es

Consortium PPPT program, called WPBB, was launched in 2014 for the development of the Breeding Blanket (BB) modules which are the structures involved in the generation of the tritium fuel essential for the operation of the plant.

In this programme [8] 4 BB options are being conceived and improved. In particular, in the present paper, two blanket concepts have been studied: the Dual-Coolant Lithium Lead (DCLL) and the Water Coolant Lithium Lead (WCLL).

The development of a DCLL BB to be integrated inside the common DEMO generic reactor is currently lead by CIEMAT [9][10]. The DCLL concept is basically characterized by the use of self-cooled breeding zones with the liquid metal LiPb serving as tritium breeder, neutron multiplier and coolant and the ferritic–martensitic steel Eurofer-97 as structural material. The WCLL concept developed currently by ENEA [12] also uses PbLi as breeder but is characterized by the use of water for cooling the Eurofer structures. More details on WCLL design are in [12][13].

From the start of the programme up to now two generic DEMO design have been conceived and analyzed being known as DEMO baseline 2014 [14] and DEMO baseline 2015 [15] (shown in figure 1a and 1b respectively). The former DEMO design had 16 sectors of 22.5º and a plasma power of 1572 MW corresponding to a 5.581×10^{20} n/s source. The present DEMO design consist of 18 sectors each one of 20º. The reactor fusion power is 2037 MW corresponding to 7.323×10^{20} n/s source. The plasma parameters (radius, elongation, triangularity, radial shift, source peaking factor) are reported in [16] for previous DEMO design and in [17] for the present one. For the neutronic studies and in the present applications, 11.5º MCNP model was used for DEMO 2014 studies and a 10º MCNP model for DEMO 2015 analyses. These represent half sectors of the 360º torus tokamak, used with reflective boundary conditions on the lateral sides to take into account full 3D transport. Baseline DEMO MCNP models are reported in Figure 1.

For DEMO 2014 the analyses have been performed using the DCLL option only. The 2014 DCLL design was fully heterogenized meaning that all the internal components of all the BB modules are represented as shown in figure 2a (showing the entire BB segmentation) and 2b (showing the DCLL OB equatorial module).

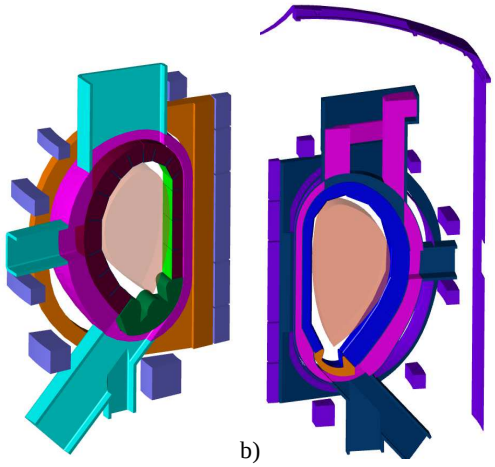

a) b)

Figure1. DEMO generic designs: a) Baseline 2014, b) Baseline 2015.

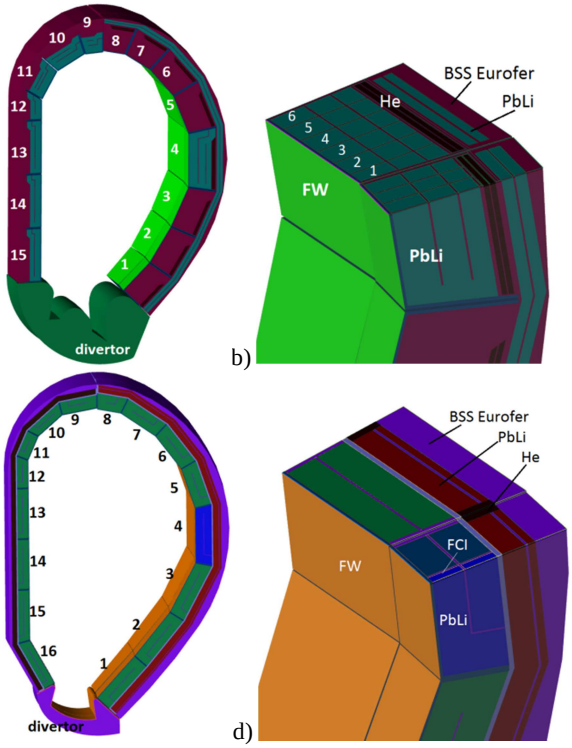

a) b) c) d)

Figure 2. DCLL: a) DEMO2014 design and b) its detailed OB equatorial module; d) DEMO2015 design with e) its detailed OB equatorial module.

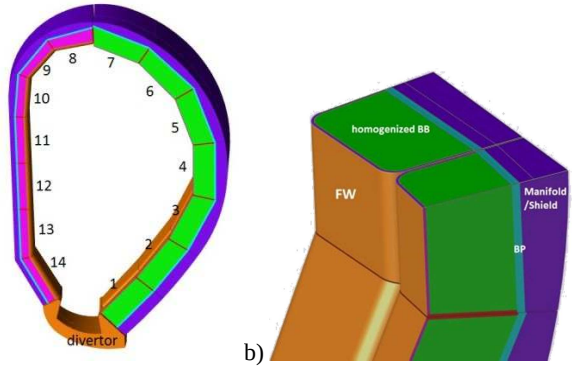

a) b)

Figure 3. a) WCLL neutronic design DEMO2015 with b) its detailed OB equatorial module.

For DEMO 2015 the two conceptual models, DCLL and WCLL, adapted to the specific feature of DEMO have been studied. The DCLL MCNP model is shown in figure 2: the DCLL BSS and BB modules' segmentation in fig. 2c and the main structures inside the equatorial OB blanket module in fig. 2d. The model is a 3D *quasi*-heterogenized design in which most of the details are included and with the equatorial OB module components (stiffening plates, flow channel inserts, breeder channels, and walls) separately described. Figure 3 shows the MCNP model of WCLL 2015: the WCLL massive BSS and BB modules' segmentation inside a sector in fig. 3a and the equatorial OB blanket module in fig. 3b. In this case an homogenized representation of the internal BB component is assumed and described as a mixture of water, PbLi and Eurofer [12][13].

2.1.2 Divertor designs

The conceptual design of the DEMO divertor was developed among the work package WPDIV 'Cassette design & integration' also launched in 2014.

At first, an ITER-like single-null divertor configuration with the divertor cassette at the bottom of the VV was considered. Strong emphasis was given in the roadmap, to identify alternative divertor configurations that alleviate the problem of excessive heat loads on the DEMO divertor targets [18].

In a second phase (2015) a revised CAD model of cassette has been created. A major design change was implemented: the outboard and inboard baffles were cut off from the cassette while the breeding blanket modules were extended to cover the previous baffle regions [19][20]. The motivation of this design change was to increase the TBR by exploiting the high dose areas of PFCs suitable for breeding. The cassette is shaped in accordance with the kinematic envelope required for remote maintenance.

In DEMO 2014 MCNP model austenitic steel (SS316LN) was considered for the divertor composition being the neutronic design [21] (see figure 1a) a block of 80%$_{vol}$ steel and 20%$_{vol}$ water homogenized mixture. This will be called in the next as "divertor #1". Such divertor DEMO2014 model occupies 10.47m^3 (in the neutronic 11.25º half-sector) corresponding to almost 66.4 Tons of steel and 2 Tons of water when using that composition.

In the way towards a major commitment to the environment, in DEMO 2015 baseline model for the divertor cassette body, as for the previous seen BB structures, the reduced activation 9Cr steel Eurofer97 has been considered as structural material. The motivation of using this steel for cassette is to exploit the essential benefits of the low activation steels to allow its disposal as a "Low Level Waste" within no more than 100 years. In the neutronic model the divertor is described as a solid steel body of Eurofer97 (called "divertor #2") except two layers facing the plasma (see figure 1b) of 5 mm thick tungsten armour, with in between a 15 mm thick tube layer filled with a homogenized mixture of 39.5% W, 17% CuCrZr, 13% Cu and 30% water. Almost 17.3 tons of Eurofer were assumed in one divertor cassette of 2.21 m^3.

In parallel, within WPDIV project a new neutronic model of divertor has been developed based on 2015 water cooled divertor cassette design. The shape is the same as in baseline model, but the composition of plasma facing components and in particular of divertor cassettes have been changed according to the last design. The assumed composition of the cassette is 28.3%$_{vol}$ Eurofer, 24%$_{vol}$ water and rest (47.7%$_{vol}$) void [22] (also equivalent to 54% Eurofer and 46% water at the reduced density of 2.43 g/cm^3). This divertor composition (called "divertor #3") has been tested for both DEMO2014 and DEMO2015 MCNP models being the first one much bigger (10.47 m^3 vs. 2.21 m^3) due to the bigger size of the cassette itself and also to the fact that a complete cassette in DEMO2015 occupies 10º instead of the 11.25º of DEMO2014. Due to these differences such composition corresponds to 4.8 Tons of Eurofer and 492 kg of water for DEMO2015 case and to 23.5Tons of Eurofer and 2.4Tons of water for DEMO2014.

The chemical compositions of the materials in all the examined configurations include all the relevant impurities because often they give rise to significant additional activation compared to the base material. The compositions considered for Eurofer97, W, PbLi, and SS316LN austenitic steel are given in [23].

2.2 The method

Particle transport calculations have been performed using Monte Carlo code MCNP5 [24] and JEFF3.1.1 [25] and JEFF3.2 [26] cross section data libraries respectively for DEMO2014 and DEMO 2015. The neutron source is described by a parametric representation of typical fusion L-mode confined plasma using an external subroutine [27] and giving the *rdum* parameters [16][17] inside the MCNP input.

For the TBR assessments the 3 MCNP models DCLL2014, DCLL2015 and WCLL2015 have been tested, each one with 2 different divertor compositions, being one its original composition as in the baseline MCNP models - divertor #1 or divertor #2 - and the other, the modified divertor #3 composition.

The neutron and gamma fluxes have been also assessed for DCLL and WCLL 2015 to demonstrate the great impact on radiation environment inside the plasma chamber due to divertor composition.

In order to calculate shutdown radiation fields the Advanced D1S method [28] has been used coupling the MCNP5 transport code with the inventory code ACAB [29] and using EAF2007 [30] as activation data library.

For shutdown dose rate (SDR) and decay gamma heating and fluxes calculations, the results are reported at 12 days after DEMO shutdown for the last DCLL2015 design only. Similar results were obtained when comparing the two different divertor compositions also for the WCLL2015 design.

The transport MCNP and activation ACAB calculations were performed on CIEMAT EULER cluster, while the AD1S calculations were performed on ENEA HPC CRESCO cluster.

The irradiation scenario assumed for the activation calculations is based on the operation scheme specified for the 1st DEMO phase [31] reaching a total of 1.57 FPY. Although the divertor could be replaced once during this time in the present simulations the replacement of the components was disregarded. This means that all the structures are exposed to the neutron irradiation during the same lifetime. The details on the set-up and application of Advanced D1S to DCLL DEMO are in [7].

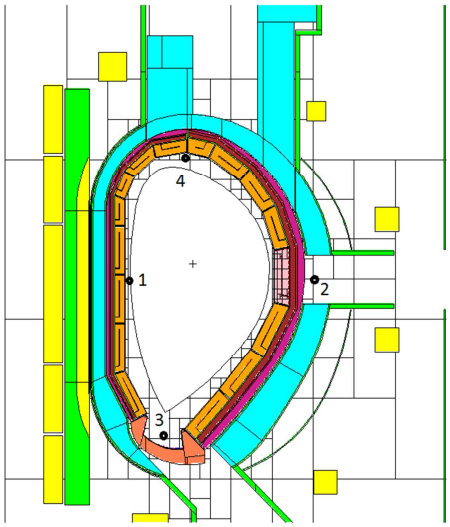

Figure. 4. MNCP DCLL DEMO model with the 4 detector in which the responses have been calculated as local values.

Specific responses and comparisons are provided at four relevant positions (see figure 4). These consist of four spherical void cells located inside the vessel in front of the inboard equatorial module (1), behind the equatorial outboard module (2), on the bottom close to the divertor (3) and on the top (4).

3. Results

3.1 Impact on the TBR

A first comparison for the tritium production between the previous divertor models and the "Eurofer-water cooled divertor" (composition #3) shows a general reduction of the breeding capabilities of the blankets modules when the water content increases inside the cassette. This is true for all the 3 DEMO models used (DCLL2014, DCLL2015 and WCLL2015).

The total TBR and its poloidal distribution among the BB modules and the BSS of the DCLL2014 and DCLL2015 are reported in tables 1 and 2, respectively, using both the originals and the new divertor. The total TBR for WCLL2015 using the two divertor compositions is reported in table 3.

When the new divertor composition (#3) is used, the loss of TBR comparing with the previous is between 2 and 5%. The highest reduction, greater than 5%, is obtained for the *quasi*-heterogenized DCLL2015 (Table 2) in which the composition has changed from full Eurofer to 28.3%$_{vol}$ Eurofer, 24%$_{vol}$ water and 47.7%$_{vol}$ void. For the fully-heterogenized DCLL2014, where the divertor composition changed from 80%$_{vol}$ Eurofer and 20%$_{vol}$ water to 28.3%$_{vol}$ Eurofer, 24%$_{vol}$ water and 47.7%$_{vol}$ void, the reduction is 3.2%. A minor impact, -2%, is found on WCLL2015 model (Table 3) because of the presence of water in homogeneous mixture used in BB modeling. In the first two cases, such loss is higher than the margin of 3% suggested to accounts for unknown uncertainties in design elements [3][4]. This would suggest revising the target TBR (1.10) in order to achieve the self-sufficiency, by increasing the design related uncertainties of in-vessel components at this status of the DEMO project.

In some of the cases the change in the divertor composition would be more critical than in other as for example for the DCLL2014 case, which although it doesn't suffer the most critical TBR loss (a 3.2%) it is subjected to the most serious reduction of TBR being from 1.104 (just above the target) to 1.07 which would imply the not fulfilment of the project requirement.

Table 1. TBR poloidal distribution in BB modules for the DCLL DEMO Baseline 2014 using the previous and new divertor compositions.

		T/n in 360º		
DCLL2014	nº	divertor #1	divertor #3	Δ%
BB OB	1	7.32E-02	7.05E-02	
	2	9.62E-02	9.32E-02	
	3	1.14E-01	1.11E-01	
	4	1.52E-01	1.48E-01	
	5	1.11E-01	1.07E-01	
	6	8.66E-02	8.41E-02	
	7	6.39E-02	6.15E-02	
	8	4.39E-02	4.24E-02	
	tot	0.7408	0.7179	
BB IB	9	3.06E-02	2.95E-02	
	10	4.66E-02	4.51E-02	
	11	3.80E-02	3.69E-02	
	12	2.28E-02	2.22E-02	
	13	5.94E-02	5.77E-02	
	14	5.78E-02	5.60E-02	
	15	4.58E-02	4.35E-02	
	tot	0.3009	0.2909	
Total BB		1.0418	1.0088	-3.26%
BSS	OB	2.50E-02	2.46E-02	
	IB	3.76E-02	3.68E-02	
	total	6.26E-02	6.13E-02	-2.04%
	TBR	**1.104**	**1.070**	-3.19%

Table 2. TBR poloidal distribution in BB modules for the DCLL DEMO Baseline 2015 using the previous and new divertor compositions.

		T/n in 360º		
DCLL2015	nº	divertor #2	divertor #3	Δ%
BB OB	1	8.81E-02	7.92E-02	
	2	1.19E-01	1.14E-01	
	3	1.42E-01	1.37E-01	
	4	1.49E-01	1.43E-01	
	5	1.08E-01	1.03E-01	
	6	9.80E-02	9.32E-02	
	7	8.25E-02	7.83E-02	
	8	4.28E-02	4.06E-02	
	tot	8.29E-01	7.87E-01	
BB IB	9	4.81E-02	4.55E-02	
	10	3.65E-02	3.46E-02	
	11	2.44E-02	2.33E-02	
	12	2.63E-02	2.51E-02	
	13	4.98E-02	4.79E-02	
	14	5.03E-02	4.83E-02	
	15	4.52E-02	4.27E-02	
	16	4.78E-02	4.35E-02	
	tot	3.28E-01	3.11E-01	
total BB		1.158	1.098	-5.4%
BSS	OB	6.93E-02	6.72E-02	
	IB	3.92E-02	3.77E-02	
	total	1.09E-01	1.05E-01	-3.49%
	TBR	**1.266**	**1.203**	-5.24%

Table 3. TBR in BB, back-plate and Manifold for the WCLL DEMO Baseline 2015 using the previous and new divertor compositions.

WCLL2015	divertor #2	divertor #3	Δ%
BB	1.135	1.113	-1.93%
Back Plate	0.0015	0.001	
Manifold	0.0134	0.0130	
TBR	**1.149**	**1.127**	-1.99%

3.1 Influence on neutron and gamma fluxes

The impact of the divertor composition on the neutron and gamma fluxes and spectra has been also assessed for the two DEMO2015 models DCLL and WCLL. As shown in Figures 5 and 6 for the global maps, but also in Figures 7 and 8 for the spectra in the bottom detector (position #3 of figure 4), the use of water coolant in the divertor implies the increase of the low energy components inside the entire plasma chamber and in its surroundings due to the great moderating power of hydrogen with the consequent increase of the neutron flux in the thermal region of the spectrum.

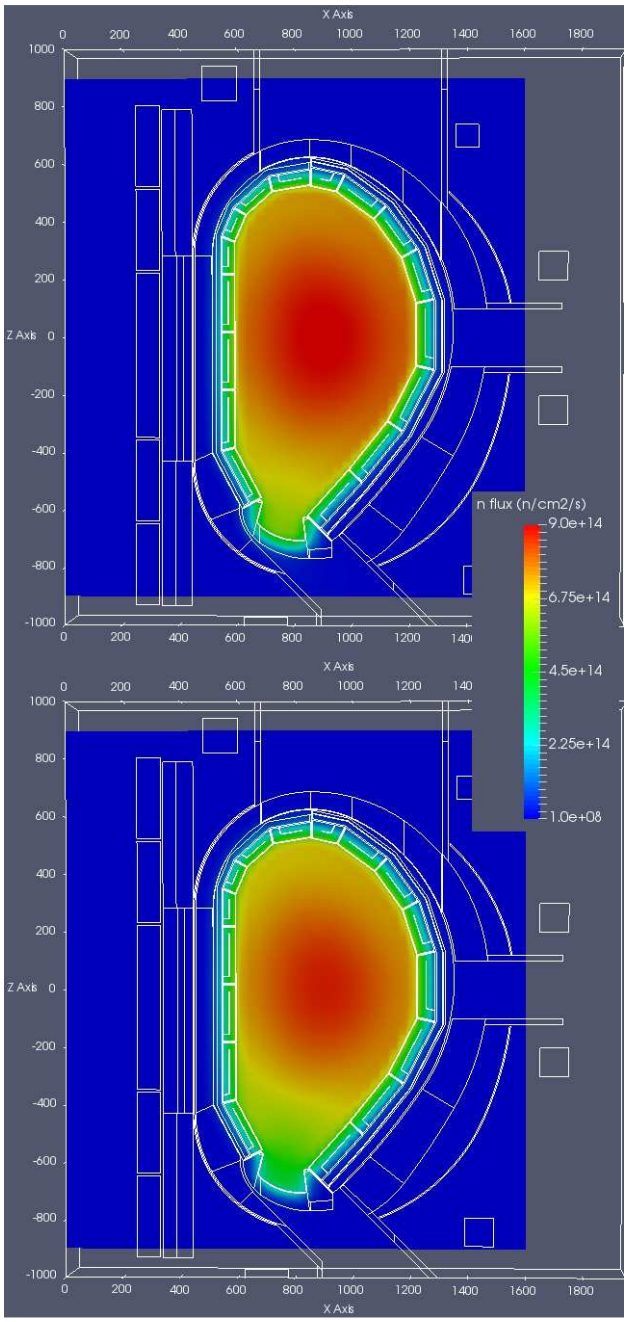

Figure 5. Neutron flux 3D maps for the DCLL DEMO2015 models with divertor #2 (up) and #3 (down) compositions.

As consequence, the heavy material (Eurofer) can absorb more easily the moderated neutrons and thus

the generated gamma flux is higher in the divertor region (see Figures 9 and 10 for the global maps, and Figures 11 and 12 for the gamma spectra in the bottom detector) due to the highest reaction rates for gamma emitting reactions.

The effect of the neutron moderation and gamma emission of the "highly water cooled" divertor composition is higher for the DCLL than for the WCLL concept. This is due to the presence of water coolant in WCLL BB system; furthermore the approximation of homogenization of breeder zone materials can also cause a mitigation of the effect of the divertor.

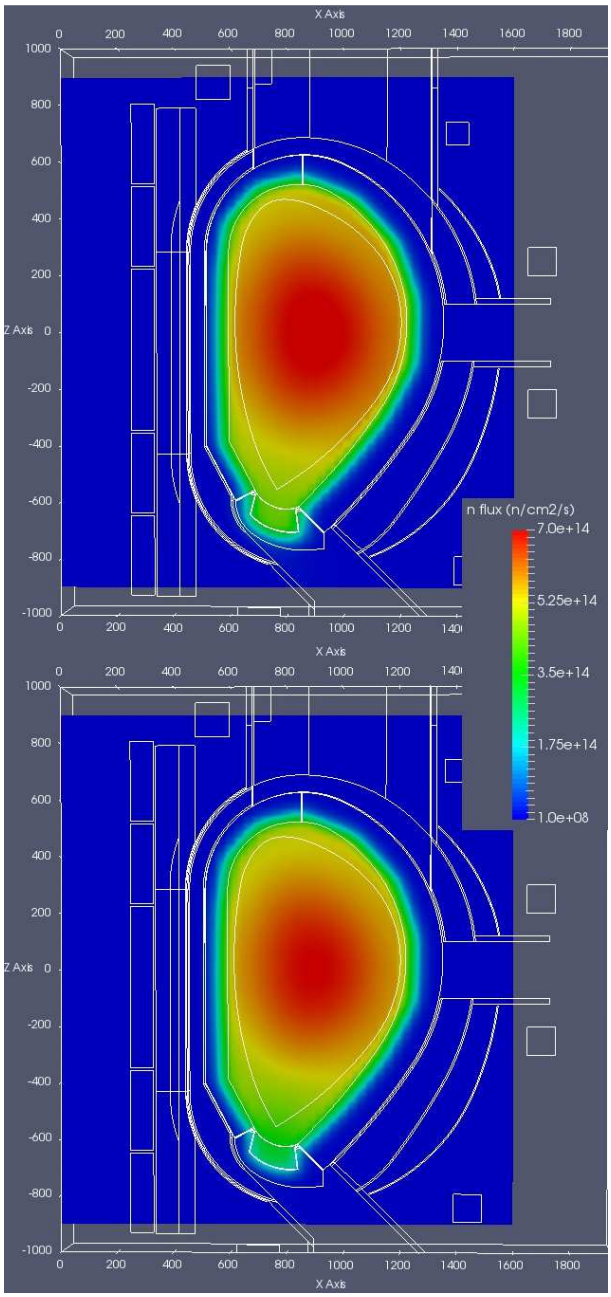

Figure 6. Neutron flux 3D maps for the WCLL DEMO2015 models with divertor #2 (up) and #3 (down) compositions.

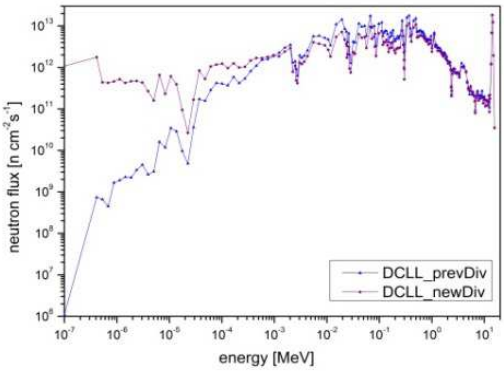

Figure 7. Neutron spectra in position #3 for the DCLL DEMO model for the 2 divertor compositions.

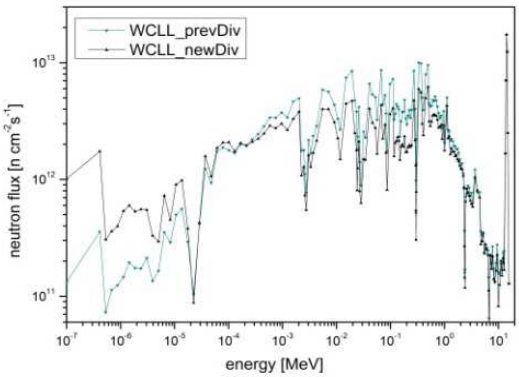

Figure 8. Neutron spectra in position #3 for the WCLL DEMO model for the 2 divertor compositions.

Table 4 Neutron and gamma fluxes at the positions 1-4 for WCLL and DCLL, and for the 2 different divertor compositions.

	WCLL		
	divertor #2	divertor #3	Δ%
pos.	neutron flux (n/cm^2/s)		
1	5.94E+14	5.74E+14	-3.30%
2	3.74E+11	3.73E+11	-0.30%
3	4.48E+14	3.21E+14	**-28.3%**
4	5.29E+14	5.10E+14	-3.48%
	gamma flux (γ/cm^2/s)		
1	1.22E+14	1.22E+14	-0.20%
2	1.03E+11	1.01E+11	-2.39%
3	8.80E+13	9.77E+13	**11.0%**
4	1.18E+14	1.17E+14	-1.05%
	DCLL		
	divertor #2	divertor #3	Δ%
pos.	neutron flux (n/cm^2/s)		
1	7.76E+14	7.35E+14	-5.33%
2	2.35E+12	2.33E+12	-0.60%
3	6.06E+14	4.27E+14	**-29.6%**
4	7.39E+14	6.99E+14	-5.40%
	gamma flux (γ/cm^2/s)		
1	1.07E+14	1.07E+14	-0.17%
2	5.98E+11	6.29E+11	5.21%
3	7.83E+13	9.62E+13	**22.8%**
4	1.05E+14	1.04E+14	-1.51%

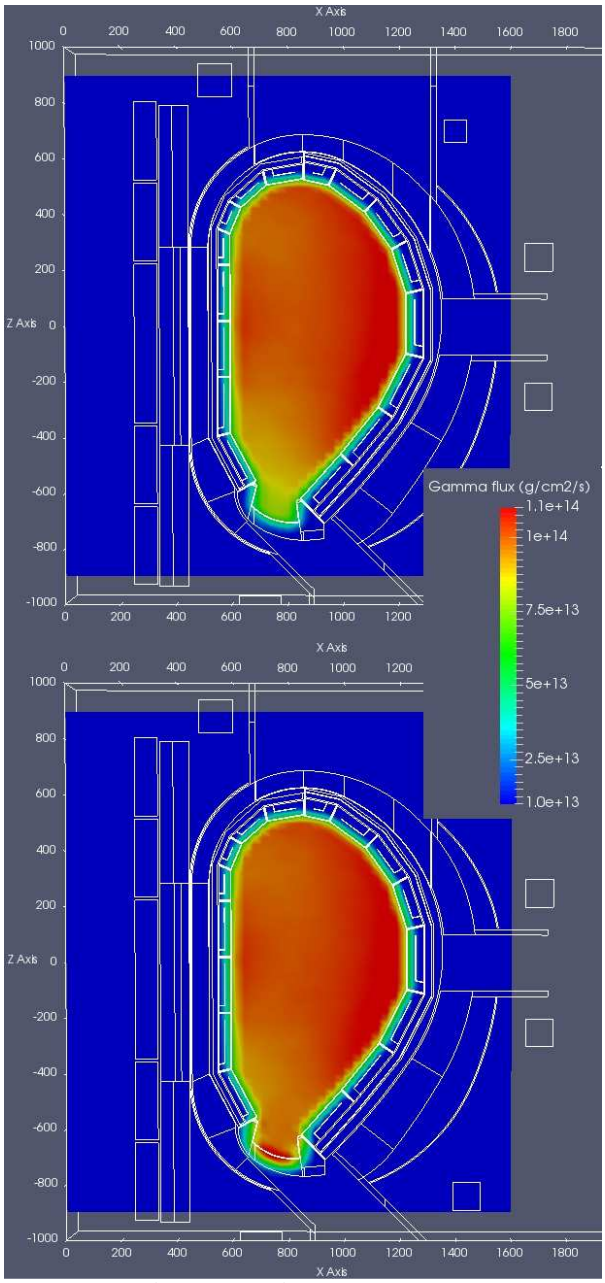

Figure 9. Gamma flux 3D maps for the DCLL DEMO models with the divertor #2 (up) and #3 (down) compositions

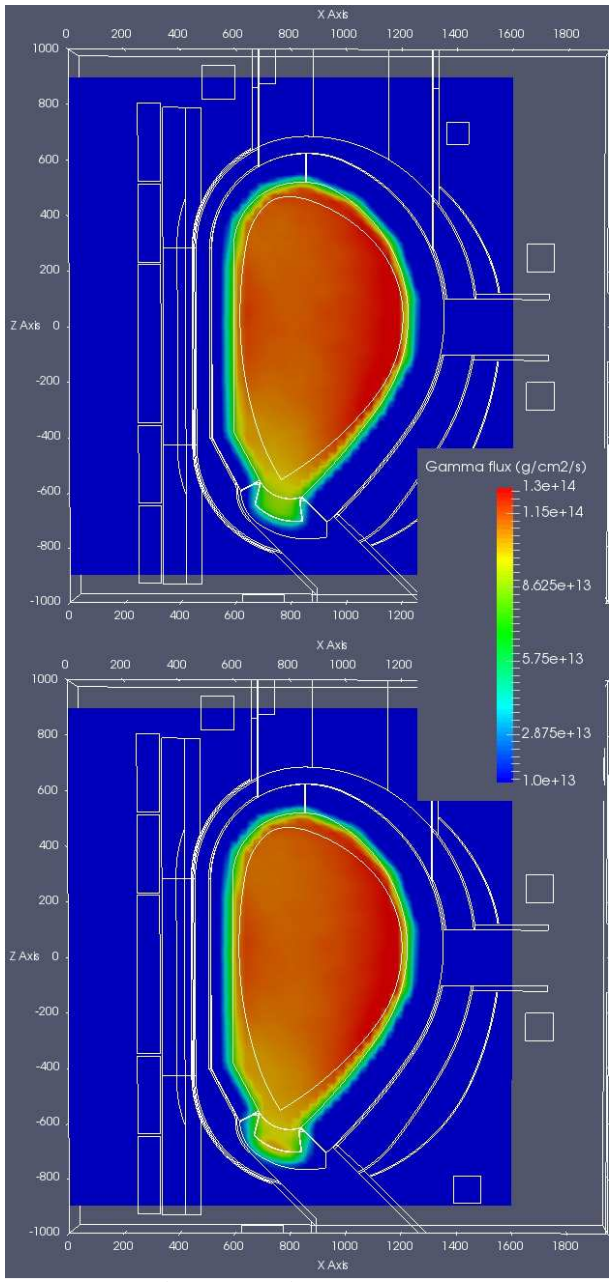

Figure 10. Gamma flux 3D maps for the WCLL DEMO models with the divertor #2 (up) and #3 (down) compositions

Table 4 reports the total neutron and gamma fluxes at the 4 positions for previous Eurofer and the recent highly water cooled divertor for both WCLL and DCLL models. The neutron total flux is reduced in all the positions for both BB concepts when the recent divertor (#3) is used due to the moderating power of water. Again it is shown in the table that such reduction is slightly higher for the DCLL than for the WCLL due to the presence of water in homogeneous mixture used in BB modeling of such concept.

Conversely, the gamma fluxes increase in position 3 (close to divertor) in both concepts although the increase is much higher for the DCLL concept (11% vs. 23%). The reduction in positions 1 and 4 is moderate for both concepts, while in the OB port detector (nº 2) an increase in the gamma flux is observed for the DCLL (5%) whereas a slight reduction is found for WCLL.

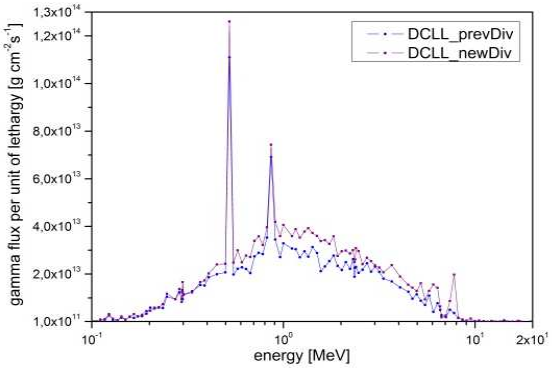

Figure 11. Gamma spectra in position #3 for the DCLL DEMO model for the 2 divertor compositions.

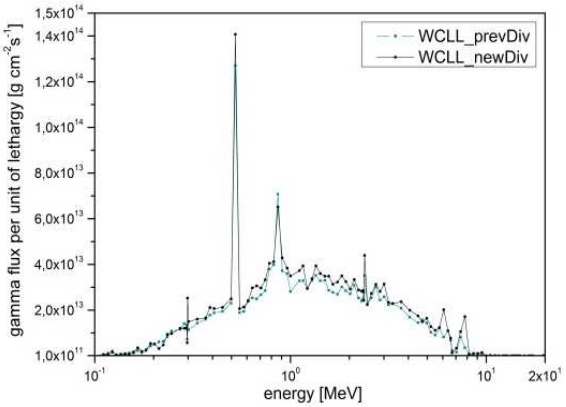

Figure 12. Gamma spectra in position #3 for the WCLL DEMO model for the 2 divertor compositions.

3.2 Impact on activation of in-vessel components

A detailed study of DCLL shutdown dose rate has been recently performed [7]. The shutdown dose rate, decay gamma fluxes, decay heat were calculated with Advanced D1S [28] coupled with ACAB [29] inventory code from 1 day to 1 year after shutdown. The study has shown that the activation of in-vessel components was also affected by divertor composition. For this reason in the present work a special focus has been given on the impact of this component also on the activation responses and thus, some results are discussed to demonstrate this thesis.

Figure 13 shows the SDR maps in the DCLL model for DEMO2015 at 12 days after shutdown for the original divertor composition (#2) and the new one (#3) with detailed pictures of the divertor zone. In Table 5 the values of SDR calculated at the four positions using the two options of divertor are presented. Decay gamma fluxes and decay gamma heating detector' values are also given.

The greatest effect due to the divertor composition is observed at the bottom position (#3), as expected, where the shutdown dose rate increases from 570 Sv/h to ≈1350 Sv/h when the water cooled divertor (#3) is used (an increase factor of 2.36). Decay gamma fluxes and decay heat increase also a factor 2.5. A moderate increase of 3-4 % is observed also at the in-vessel positions 1 and 4. The OB in-port position (2) shows a weak reduction of all the responses.

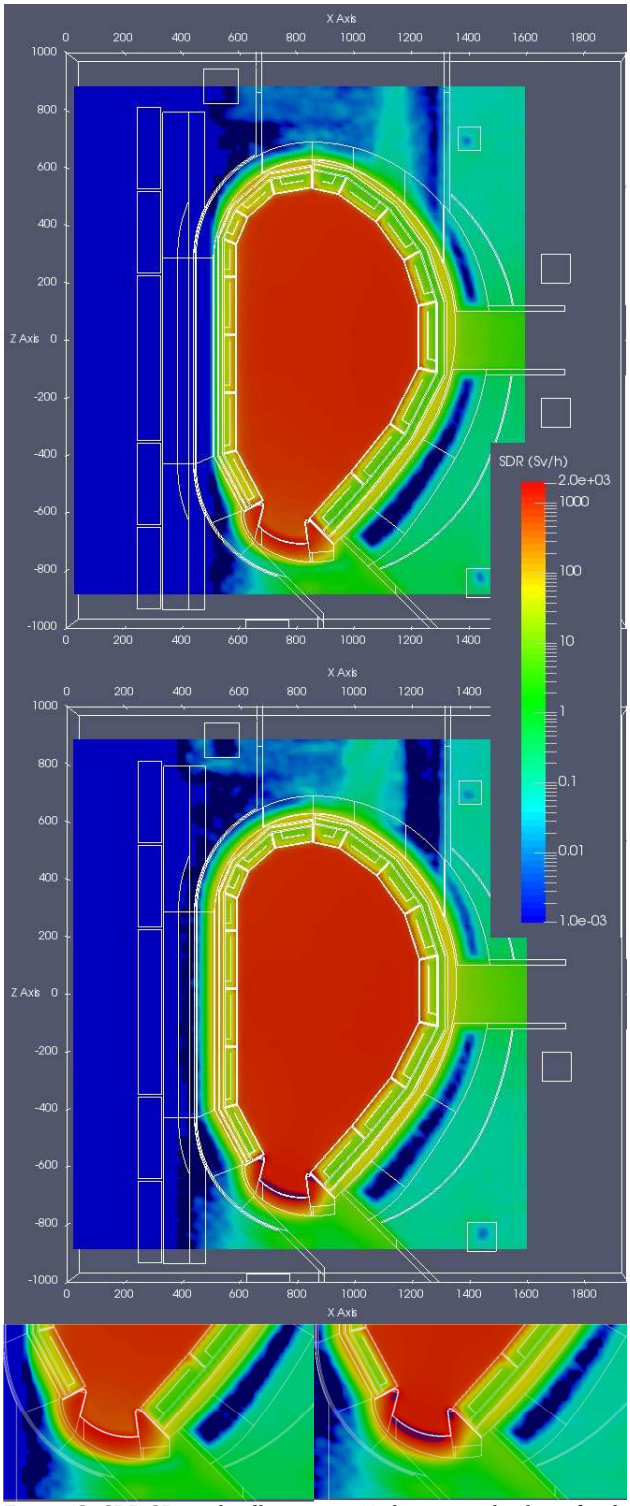

Figure 13: SDR 3D mesh tally maps at 12 days since shutdown for the DCLL DEMO2015 model comparing divertor #2 (up) and #3 (down).Values outside the adopted scale are in deep-blue (under the scale) and deep-purple (over the scale) colours.

Figure 14 shows the major contributions to the total SDR. At 12 days after shutdown, gammas from the decay of Co-58, Co-60, Mn-54, Ta-182 and Fe-59 were identified as the dominant contributors to the doses. The major contributors to the SDR in positions 1, 3 and 4 are Mn-54 ($T_{1/2}$ ~312 days) and Ta-182 ($T_{1/2}$ ~115 days) and in position 2 the dominants are Ta-182 and Co-60 ($T_{1/2}$ ~5.27 years). The Mn-54 is generated mainly from Fe-54 (n,p) and Mn-55 (n,2n) reactions. The use of a different divertor composition is reflected not only in the total SDR but also in the different contributors to the SDR. With the full Eurofer divertor the contributors to dose in position 3 are mainly Mn54 (63%) and Ta182 (32%) while using the recent water cooled steel divertor composition, besides Ta182 (40%) and Mn54 (25%), Co-60 also provides a relevant contribution (32%).

Table 5. Shutdown dose rate, decay gamma flux and decay heat at 12 days after DEMO shutdown at the positions 1-4 and for the 2 different divertor compositions.

	Shutdown dose rate (Sv/h)		
pos	Full-Eurofer Divertor #2	Eurofer-Water cooled Divertor #3	Δ%
1	1.05E+03	1.10E+03	4.26%
2	1.58E+01	1.56E+01	-1.62%
3	5.70E+02	1.35E+03	136.4%
4	1.00E+03	1.05E+03	4.67%
	Decay gamma flux (γ/cm^2/s)		
pos	Full-Eurofer Divertor #2	Eurofer-Water cooled Divertor #3	Δ%
1	9.00E+10	9.40E+10	4.51%
2	1.43E+09	1.42E+09	-0.61%
3	4.66E+10	1.19E+11	154.6%
4	8.58E+10	9.00E+10	4.88%
	Decay Heat (W/cm^3)		
pos	Full-Eurofer Divertor #2	Eurofer-Water cooled Divertor #3	Δ%
1	2.35E-03	2.45E-03	4.42%
2	3.78E-05	3.72E-05	-1.48%
3	1.32E-03	3.06E-03	132.9%
4	2.27E-03	2.35E-03	3.73%

An increase of Co-60 contribution (red bar in figure 14) when using the new divertor is observed in all in-vessel positions. Indeed in position 1, the Co-60 contribution increases from 2.68 to 23.4 Sv/h (an increase of one order of magnitude) and in position 4 from 3.41 to 17.8 Sv/h (a factor 5), respectively with the original and new compositions.

The differences in Co-60 due to the divertor are also highlighted in Figures 15 and 16 which show the total decay gamma spectra in the 4 positions (Figure 15) for the 2 divertors and the specific contribution due to Co-60 for both compositions, in position 1 (IB equatorial – Figure 16a) and 3 (Bottom- Figure 16b), respectively. The profiles again indicate that the divertor composition influences mainly but not only its surroundings but also the proximity of the IB equatorial zone due to the increase of Co-59 (n,g) and Ni-60 (n,p) reaction rates.

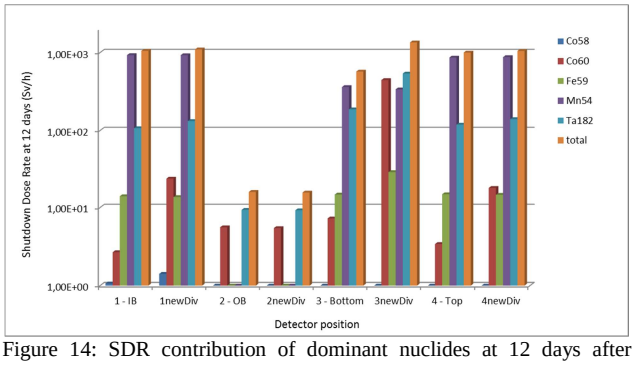

Figure 14: SDR contribution of dominant nuclides at 12 days after shutdown for the 2 divertor compositions and at 4 different locations.

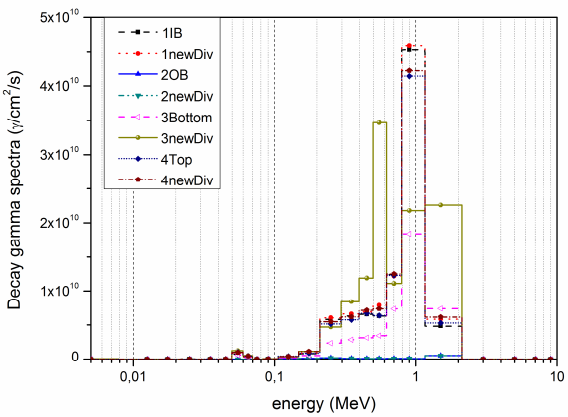

Figure 15. Decay gamma spectra (γ/cm^2/s) at the four detector positions at 12 days after shutdown.

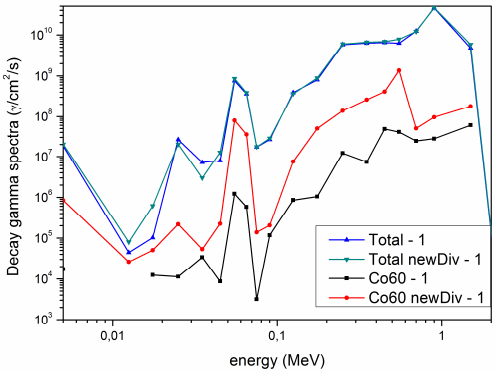

a)

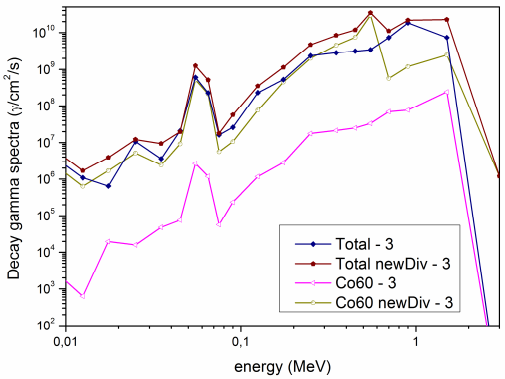

b)

Figure 16. Decay gamma spectra (γ/cm^2/s) in position IB equatorial (1) and Bottom (3) with specific profiles for Co60 contribution.

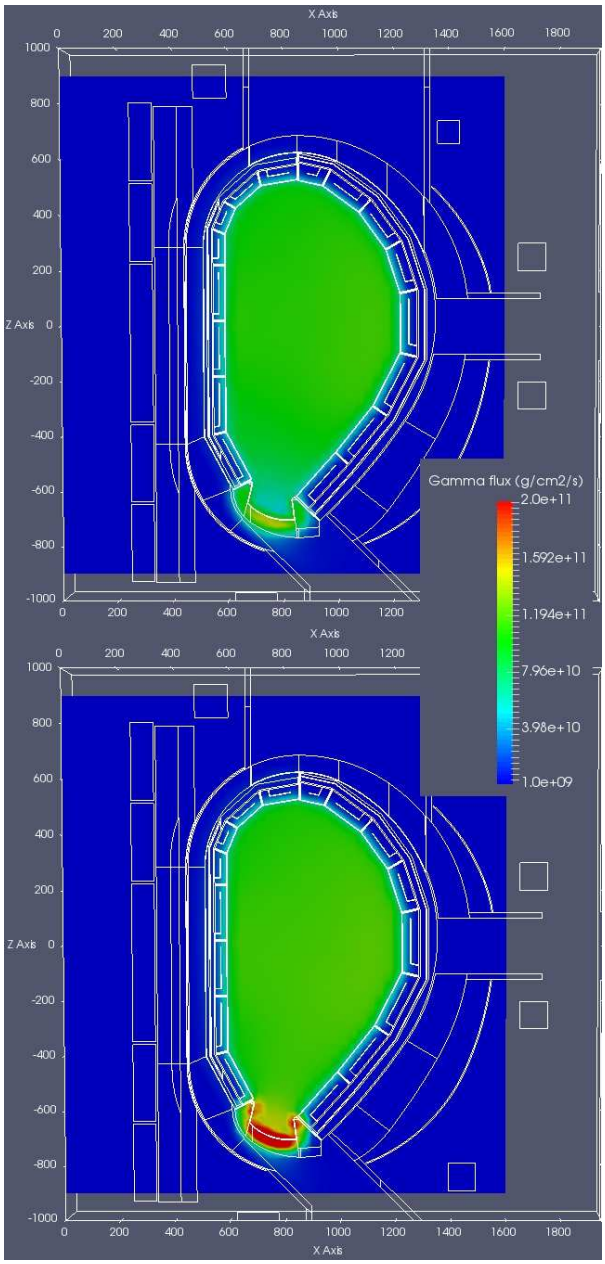

Figure 17. Decay gamma flux 3D maps at 12 days since shutdown for the DCLL DEMO model with divertor #2 (up) and #3 (down).

Looking at the spectral shape in position 3 (Figure 15) two intense peaks in the energy bins 0.5-0.6 and 1-2 MeV are observed with the new watered divertor composition, not present when the previous full Eurofer divertor is used. According to the specific Co-60 profiles (Figure 16) it is possible to observe such increase of the decay gamma at 0.5-0.6 MeV when the new divertor is used (and in both position 1 and 3). The peak in the energy range 1-2 MeV is mainly due to Ta-182 which contribution increase in such position when divertor #3 is used.

According to the mesh results of Figure 17 and also to the specific values given in Table 5 the decay gamma flux ranges between $\approx 4.7 \times 10^{10}$ and $\approx 1.2 \times 10^{11}$ $\gamma/cm^2/s$ inside the port vessel around position 3 depending on the divertor considered.

The decay gamma heating on Eurofer components has been also calculated both as 3D maps (Figure 18) and as local value in the detector positions (Table 5). The maximum decay heat on Eurofer is $\approx 3 \times 10^{-3}$ W/cm^3 on the divertor when the new composition with water is used, while $\approx 1 \times 10^{-3}$ W/cm^3 is the result when the original one is adopted. Again a difference of a factor ≈2.5 is observed for this global result as for the other 2 responses (decay γ flux and SDR).

Figure 18: Decay gamma heating in Eurofer at 12 days after shutdown for the DCLL DEMO model with divertor #2 (up) and #3 (down). Values outside the adopted scale are in deep-blue and deep-purple colours.

4. Conclusions

The analyses described in the paper have demonstrated that the divertor composition has some impact on the TBR.

The use of a different divertor design could seriously compromise the tritium breeding capabilities of a given DEMO reactor.

Preliminary results have shown that, according to the BB concept and employed homogenizations in there, a reduction between 2 and 5% could be produced when the water content inside the steel divertor cassette is increased and the amount of steel is reduced. In fact when the cassette change from 80%$_{vol}$ Eurofer and 20%$_{vol}$ water (divertor #1) mixture to 28.3%$_{vol}$ Eurofer, 24.0%$_{vol}$ water and 47.7%$_{vol}$ void (divertor #3) - that means a factor 2.8 of steel reduction (from 66.4 to 23.5 Tons) and an increase of water content (from 2 to 2.4 Tons) - the reduction of the DCLL TBR is of 3%.

When it changes from a 100% Eurofer (divertor #2) to 28.3%$_{vol}$ Eurofer, 24.0%$_{vol}$ water and 47.7%$_{vol}$ void (divertor #3) – that means a factor 3.5 of steel reduction (from 17.3 to 4.8 Tons) and a strong increase in water content (from 0 to 492 Kg) - the loss of TBR is 5% in the heterogenized DCLL and 2% in the homogenized WCLL.

The neutron and gamma fields inside the plasma chamber and in the surrounding plasma facing zones are also strongly conditioned by the choice of material composition in the divertor.

A great impact of the divertor composition is shown also on activation responses. A general increase of shutdown dose rate, decay gamma heating and flux of about a factor 2.5 in the position closest to the divertor is observed when the Eurofer-water cooled composition is used compared with full Eurofer divertor. The main responsible is the Co-60 which contribution to the SDR increases ≈60 times close to divertor. The activation in other in-vessel positions (Top and IB eq. plasma detectors) also shows a moderate increase of the local SDR due to Co-60.

Further studies will be carried-out using a detailed heterogeneous model of divertor based on recent design studies.

Acknowledgments

This work has been carried out within the framework of the EUROfusion Consortium and has received funding from the Euratom research and training programme 2014-2018 under grant agreement No 633053. The views and opinions expressed herein do not necessarily reflect those of the European Commission. The support from the EUROfusion Researcher Fellowship programme under the task agreement AWP15-ERG-CIEMAT/Palermo is gratefully acknowledged. The work has been partially supported by Spanish MINECO, HISMEFUS project ENE2013-43650-R, and by Comunidad de Madrid under TECHNOFUSION(II)-CM, S2013/MAE-2745.

The computing resources and the related technical support used for this work have been provided by CRESCO/ENEAGRID High Performance Computing infrastructure and its staff [32]. CRESCO/ENEAGRID High Performance Computing infrastructure is funded by ENEA, the Italian National Agency for New Technologies, Energy and Sustainable Economic Development and by Italian and European research programmes, see http://www.cresco.enea.it/english for information.

References

[1] M. A. Abdou, E. L. Vold, C. Y. Gung, M. Z. Youssef, K. Shin, Deuterium-Tritium Fuel Self-Sufficiency in Fusion Reactors, Fusion Science and Technology, Volume 9 (1986) 250-285

[2] M.E. Sawan, M.A. Abdou, Physics and technology conditions for attaining tritium self-sufficiency for the DT fuel cycle, Fusion Eng. Des. 81 (2006) 1131–1144

[3] L. El-Guebaly, S. Malang, Towards the ultimate goal of tritium self-sufficiency:technical issues and requirements imposed on ARIES advanced power plants, Fusion Eng. Des. 84 (2009) 2072–2083.

[4] U. Fischer, C. Bachmann, I. Palermo, P. Pereslavtsev, R. Villari, Neutronics requirements for a DEMO fusion power plant, Fusion Eng. Des. 98–99 (2015) 2134–2137

[5] Shanliang Zheng, Thomas N. Todd, Study of impacts on tritium breeding ratio of a fusion DEMO reactor, Fusion Eng. Des. 98–99 (2015) 1915-1918

[6] P. Pereslavtsev et al., Analyses of Generic Issues Affecting the TritiumBreeding Performance in Different DEMO Blanket Concepts, Fusion Eng. Des. 109–111 (2016) 1207–1211

[7] I. Palermo, R. Villari, A. Ibarra, Shutdown dose rate assessment with the Advanced D1S method for the European DCLL DEMO, submitted to Fus. Eng. Des.

[8] Boccaccini L.V. *et al.*, Objectives and status of EUROfusion DEMO blanket studies, Fus. Eng. Des. (2015), http://dx.doi.org/10.1016/j.fusengdes.2015.12.054

[9] Rapisarda D. *et al.*, Conceptual Design of the EU-DEMO Dual Coolant Lithium Lead Equatorial Module, Transactions On Plasma Science http://dx.doi.org/10.1109/TPS.2016.2561204

[10] Palermo I. *et al.*, Neutronic analyses of the preliminary design of a DCLL blanket for the EUROfusion DEMO power plant, Fus. Eng. Des. http://dx.doi.org/10.1016/j.fusengdes.2016.03.065

[11] Iole Palermo, David Rapisarda, Iván Fernández-Berceruelo, Angel Ibarra, Optimization process for the design of the DCLL blanket for the European DEMOnstration fusion reactor according to its nuclear performances (Nuclear Fusion, preceeding IAEA 2016)

[12] A. Del Nevo, et al., EFDA_D_2N6WLQ v1.0 - Internal Deliverable BB-3.2.1-T002-D001: WCLL Design Report 2015

[13] A. Del Nevo et.al., WCLL breeding blanket design and integration for DEMO 2015: status and perspectives, submitted to Fus. Eng. Des.

[14] Meszaros B, DEMO CAD model modifications 2013/2014 EFDA_D _2D4NYN v1.2 April 2014

[15] Wenninger R., DEMO1 Reference Design - "EU DEMO1 2015" https://idm.euro-fusion.org/?uid=2LBJRY

[16] Kemp R, DEMO1_July_12, EFDA_D_2LBVXZ v1.0, (2012)

[17] Pereslavtsev P., 2015 Generic DEMO Model for MCNP, https://idm.euro-fusion.org/?uid=2L6HJ7

[18] C. Bachmann, et al., Initial DEMO tokamak design configuration studies, Fus. Eng. Des. 98–99 (2015) 1423–1426

[19] C. Bachmann, et al., Issues and strategies for DEMO in-vessel component integration, Fusion Eng. Des. 112 (2016) 527–534

[20] J.H. You, et al., Conceptual design studies for the European DEMO divertor: Rationale and first results, Fusion Eng. Des. 109–111 (2016) 1598-1603

[21] Iole Palermo, Iván Fernández, David Rapisarda, Angel Ibarra, Neutronic analyses of the preliminary design of a DCLL blanket for the EUROfusion DEMO power plant, Fusion Eng. Des. 109–111 (2016) 13–19

[22] R. Villari, Neutronic Analysis Report for Divertor Cassette and PFC 2015, EFDA_D_2MN2H3 v1.0 June 2016

[23] U. Fischer, Guidelines for neutronic analyses, EFDA_D_2L8TR9 v1.5 (2016)

[24] X-5 Monte Carlo Team, 'MCNP – A general Monte Carlo N-Particle Transport Code, Version 5'

[25] The JEFF-3.1.1 Nuclear Data Library, JEFF Report 22, OECD (2009) NEA No. 6807.

[26] The JEFF-3.2 Nuclear Data Library, http://www.oecd-nea.org/dbforms/data/eva/evatapes/jeff_32/ NUCLEAR ENERGY AGENCY, OECD

[27] EFDA, 'DEMO1 Source subroutine in FORTRAN90,EFDA D 2MH7CP.B (2013)

[28] R. Villari, U. Fischer, F. Moro, P. Pereslavtsev, L. Petrizzi, S. Podda, A. Serikov, shutdown dose rate assessment with the Advanced D1S method: Development, applications and validation, Fusion Engineering and Design 89 (2014) 2083–2087

[29] J. Sanz, O. Cabellos, N. Garria-Herranz, ACAB-2008, ACtivation ABacus Code V2008, NEA Data Bank (NEA-1839), 2009

[30] R.A. Forrest, J. Kopecky, J.-Ch. Sublet, The European Activation File: EAF-2007 neutron-induced cross section library, UKAEA FUS 535, March 2007

[31] J. Harman, WP12 DEMO Operational Concept Description, https://idm.euro-fusion.org/?uid=2LCY7A EFDA 2LCY7A 2012

[32] G. Ponti et al., "The role of medium size facilities in the HPC ecosystem: the case of the new CRESCO4 cluster integrated in the ENEAGRID infrastructure", Proceedings of the 2014 International Conference on High Performance Computing and Simulation, HPCS 2014, art. no. 6903807, 1030-1033;